PHYSICAL REVIEW D **92,** 053011 (2015)

Higgs boson structure functions as signposts of new physics

G. J. Gounaris[1] and F. M. Renard[2]

[1]*Department of Theoretical Physics, Aristotle University of Thessaloniki, Gr-54124 Thessaloniki, Greece*
[2]*Laboratoire Univers et Particules de Montpellier, UMR 5299 Université Montpellier II, Place Eugène Bataillon CC072 F-34095 Montpellier Cedex 5, France*

(Received 3 August 2015; published 22 September 2015)

We show that the Higgs boson structure functions observable in the inclusive process $e^-e^+ \to H +$ "anything", may reveal the presence of anomalous contributions corresponding to several types of new physics partners, Higgs boson compositeness, or invisible (dark) matter. This could be done without making a difficult or even an impossible experimental analysis of what "anything" contains. We give illustrations showing how the shapes of the various structure functions induced by such new contributions may differ from the standard predictions, thus possibly allowing their identification.

DOI: 10.1103/PhysRevD.92.053011 PACS numbers: 12.15.-y, 12.60.-i, 13.66.Fg

I. INTRODUCTION

The discovery [1] of the Higgs boson [2] is a great step towards the verification of the standard model (SM) [3]. Nevertheless there are several experimental (muon g-2, neutrino masses, dark matter) and theoretical (hierarchy problem,…) points which are not covered by SM [4]. Many ways, of very different nature, have been proposed for making a fruitful extension of SM, like supersymmetry, additional strong sectors, compositeness, and dark sectors, globally called "beyond the standard model" (BSM) [5].

Here we want to turn in particular to the difficulty in analyzing the mechanisms responsible for producing multiparticle or invisible states, in particular dark matter, in association with the Higgs particle. Indeed, the Higgs boson may couple to several new particles and may be a portal to such new sectors [6]. So we thought that a possible hint may arise if we look at the "Higgs structure functions" in the *inclusive* process $e^-e^+ \to H(p_H^\mu) + X$, where p_H^μ denotes the H-four-momentum, s describes the total e^-e^+ c.m. energy-squared, and X stands for an additional final state with two or more particles. We ignore contributions where X is a single particle associated to H (for example $e^-e^+ \to HZ$) since it is localized at a single point near the end of the spectrum, with the c.m. H-energy being $p_H^0 = (s + m_H^2 - m_Z^2)/(2\sqrt{s})$. Instead, we are rather interested by the shapes of the structure functions versus s and p_H.

At the LHC, there may also be other similar inclusive processes, where the Higgs-particle is produced in association with new particles. But in this paper we only consider the e^-e^+ process, which is probably the simplest and clearest one phenomenologically.

In particular, if the X-state mentioned above is generated through an s-channel intermediate state ($V = \gamma,\ Z$), as in

$$e^-e^+ \to V(\gamma, Z) \to H(p_H^\mu) + X, \qquad (1)$$

which is true for the BSM models used here and partly also for SM, then the general form of the cross section for any e^-e^+-polarizations, may be described by just three structure functions W_i ($i = 1, 2, 3$). These W_i functions may then be chosen to depend only on s and the c.m. magnitude of the H momentum [7].

In Sec. II we give the definitions of these functions and recall the relations among the three W_i, induced by the quantum numbers of the particles associated to the H production. In Sec. III we show how they can be simply measured through the angular distribution of the H-inclusive cross section in the e^-e^+ unpolarized and polarized cases. In Sec. IV we compute their standard contributions, where the 2-body X ("anything") state associated to H, is due to the usual fermion pairs ($t\bar{t}$ and the light $f\bar{f}$ ones) and the ZH bosons.

We treat separately the case $X = W^-W^+$, which can only partly be described by the form (1), since now one has to add the t-channel neutrino exchange amplitude, followed by a $W^\mp W^\pm H$ coupling. We also include separately the similar t- and u- channel electron exchange processes $e^-e^+ \to ZZ$ and $e^-e^+ \to Z\gamma$ followed by a ZZH coupling.

For simplicity, we ignore the contributions of the ZZ and W^-W^+ fusion processes $e^-e^+ \to e^-e^+H$ and $e^-e^+ \to \nu_e\bar{\nu}_e H$ (see [8]), since these processes can be considered as a "background" which may be subtracted from the data,[1] before making the analysis we propose.

In Sec. V we then give typical examples of possible new physics contributions; i.e. production of new bosons or fermions emitting the Higgs boson, either in the form of additional associated 2-body contributions of type (1) or in a form similar to the hadronic parton model in the case of Higgs boson compositeness. We then show how the structure functions W_i depend on the nature of the associated particles and on their parameters (masses,

[1]See Sec. IV.

couplings). In particular we show how the shapes of the s and p_H dependencies of the various W_i are affected by the nature of the associated particles, which are generally difficult to detect directly. Several illustrations for the various combinations of these structure functions are given.

Summarizing, the contents of the paper are the following. In Sec. II we give the precise definition of the structure functions. In Sec. III we express their measurability through the angular dependencies of the polarized and unpolarized cross sections. Section IV is devoted to the theoretical computation and illustrations of the SM contributions to the structure functions, while Sec. V concentrates in some examples of new physics effects. Conclusions mentioning possible future developments are given in Sec. VI.

II. STRUCTURE FUNCTIONS

The cross section of the process (1) may be written as [7]

$$\sigma = \frac{(2\pi)^4}{2s}\int d\rho L^{\alpha\beta}_{\mu\nu} H^{\mu\nu}_{\alpha\beta}, \tag{2}$$

where $L^{\alpha\beta}_{\mu\nu}$ arise from the square of the initial vertex and the γ, Z propagators, while $H^{\mu\nu}_{\alpha\beta}$ comes from the final part $\gamma, Z \to H + X$, containing the Higgs structure functions; α, β refer to γ or Z. Denoting by p^μ_H the four-momentum of the final H-particle and by q^ν the e^-e^+-total four-momentum, we define

$$d\rho = \frac{d_3 p_H}{2(2\pi)^3 p^0_H} d\rho_X, \tag{3}$$

with $d\rho_X$ containing the phase-space of the final X-state. Using this, one writes

$$\begin{aligned}\int d\rho_X H^{\mu\nu}_{\alpha\beta} &= \frac{1}{(2\pi)^3} W^{\mu\nu}_{\alpha\beta} = \sum_i I^{\mu\nu}_i W^{\alpha\beta}_i \\ &= -\left(g^{\mu\nu} - \frac{q^\mu q^\nu}{s}\right) W^{\alpha\beta}_1 + \left(p^\mu_H - \frac{p_H.q}{s} q^\mu\right) \\ &\quad \times \left(p^\nu_H - \frac{p_H.q}{s} q^\nu\right) \frac{W^{\alpha\beta}_2}{m^2_H} - i\epsilon^{\mu\nu\rho\sigma} p_{H\rho} q_\sigma \frac{W^{\alpha\beta}_3}{m^2_H},\end{aligned} \tag{4}$$

where

$$\begin{aligned} I_1 &= -\left(g^{\mu\nu} - \frac{q^\mu q^\nu}{s}\right), \\ I_2 &= \frac{1}{m^2_H}\left(p^\mu_H - \frac{p_H.q}{s} q^\mu\right)\left(p^\nu_H - \frac{p_H.q}{s} q^\nu\right), \\ I_3 &= \frac{-i}{m^2_H}\epsilon^{\mu\nu\rho\sigma} p_{H\rho} q_\sigma \end{aligned} \tag{5}$$

are the only terms that remain nonvanishing after contracting with $L^{\alpha\beta}_{\mu\nu}$; compare (2). Note that the H structure functions $W^{\alpha\beta}_i$ in (4), are taken as functions of $s = q^2$ and the c.m. magnitude of the H momentum

$$p_H = \frac{\sqrt{[s - (m_H + M_X)^2][s - (m_H - M_X)^2]}}{2\sqrt{s}}, \tag{6}$$

where M_X denotes the invariant mass of the X-state. As a first step we only consider 2-body X-states. At very high energies, multibody X contributions would probably also be needed.

A. H + 2-body contributions

We start from the transition $\gamma, Z \to x + x'$ followed by $x \to x'' + H$ or $x' \to x'' + H$, where x, x', x'' can be scalars, fermions or gauge bosons. For each X, one squares the sum over all diagrams, obtaining an expression for $H^{\mu\nu}_{\alpha\beta}$. We then compute its corresponding three numerical quantities,

$$K^{\alpha\beta}_i = \int d\rho_X H^{\mu\nu}_{\alpha\beta} I^{\mu\nu}_i, \tag{7}$$

by integrating the $I^{\mu\nu}_i$ expressions in (5). Denoting the respective momenta of (x', x'') as (p', p''), we have

$$d\rho_X = \frac{1}{4(2\pi)^6}\frac{d_3 p' d_3 p''}{p'^0 p''^0}\delta_4(q - p_H - p' - p''), \tag{8}$$

which through (4) lead to

$$\begin{aligned} W^{\alpha\beta}_1 &= \frac{s m^2_H}{2[s m^2_H - (p_H.q)^2]}\left[\frac{K^{\alpha\beta}_1}{s m^2_H}[s m^2_H - (p_H.q)^2] + K^{\alpha\beta}_2\right], \\ W^{\alpha\beta}_2 &= \frac{s^2 m^4_H}{2[s m^2_H - (p_H.q)^2]^2}\left[\frac{K^{\alpha\beta}_1}{s m^2_H}[s m^2_H - (p_H.q)^2] + 3K^{\alpha\beta}_2\right], \\ W^{\alpha\beta}_3 &= \frac{m^4_H}{2[s m^2_H - (p_H.q)^2]} K^{\alpha\beta}_3. \end{aligned} \tag{9}$$

III. THE e^-e^+ CROSS SECTION

Using (2)–(5) and $\alpha = e^2/(4\pi)$, the general inclusive cross section for polarized $e^\mp$ beams is written as

$$\begin{aligned}&\frac{p^0_H d\sigma(e^-e^+ \to H + X)}{d_3 p_H} \\ &= \frac{\alpha^2}{s^2}\{(1 - P_L P'_L)U_1 + (P_L - P'_L)U_2 \\ &\quad + P_T P'_T(U_3 \cos 2\phi + U_4 \sin 2\phi)\},\end{aligned} \tag{10}$$

where P_L, $P_{L'}$, P_T, $P_{T'}$ are the longitudinal and transverse $e^\mp$ beam degrees of polarization and

$$
\begin{aligned}
U_1 &= \left(W_1^{\gamma\gamma} + \frac{p_H^2}{2m_H^2} W_2^{\gamma\gamma}\sin^2\theta\right) + \frac{s^2(|g_{Zee}^L|^2 + |g_{Zee}^R|^2)}{2(s-m_Z^2)^2}\left(W_1^{ZZ} + \frac{p_H^2}{2m_H^2} W_2^{ZZ}\sin^2\theta\right) \\
&\quad - \mathrm{Re}\left\{\frac{s(g_{Zee}^{L*} + g_{Zee}^{R*})}{(s-m_Z^2)}\left(W_1^{\gamma Z} + \frac{p_H^2}{2m_H^2} W_2^{\gamma Z}\sin^2\theta\right)\right\} \\
&\quad + \frac{s^2(|g_{Zee}^L|^2 - |g_{Zee}^R|^2)p_H\sqrt{s}}{2(s-m_Z^2)^2 m_H^2} W_3^{ZZ}\cos\theta + \mathrm{Re}\left\{\frac{s(g_{Zee}^{R*} - g_{Zee}^{L*})p_H\sqrt{s}}{(s-m_Z^2)m_H^2} W_3^{\gamma Z}\right\}\cos\theta, \\
U_2 &= \frac{s^2(|g_{Zee}^L|^2 - |g_{Zee}^R|^2)}{2(s-m_Z^2)^2}\left(W_1^{ZZ} + \frac{p_H^2}{2m_H^2} W_2^{ZZ}\sin^2\theta\right) + \mathrm{Re}\left\{\frac{s(g_{Zee}^{R*} - g_{Zee}^{L*})}{(s-m_Z^2)}\left(W_1^{\gamma Z} + \frac{p_H^2}{2m_H^2} W_2^{\gamma Z}\sin^2\theta\right)\right\} \\
&\quad + \frac{s^2(|g_{Zee}^L|^2 + |g_{Zee}^R|^2)p_H\sqrt{s}}{2(s-m_Z^2)^2 m_H^2} W_3^{ZZ}\cos\theta - \mathrm{Re}\left\{\frac{s(g_{Zee}^{L*} + g_{Zee}^{R*})p_H\sqrt{s}}{(s-m_Z^2)m_H^2} W_3^{\gamma Z}\right\}\cos\theta, \\
U_3 &= \frac{-p_H^2}{2m_H^2} W_2^{\gamma\gamma}\sin^2\theta - 2\frac{s^2\mathrm{Re}\{g_{Zee}^L g_{Zee}^R\}p_H^2}{2m_H^2(s-m_Z^2)^2} W_2^{ZZ}\sin^2\theta + \frac{p_H^2\mathrm{Re}\{s(g_{Zee}^{L*} + g_{Zee}^{R*})W_2^{\gamma Z}\}}{2m_H^2(s-m_Z^2)}\sin^2\theta, \\
U_4 &= -\frac{p_H^2\mathrm{Im}\{s(g_{Zee}^{L*} - g_{Zee}^{R*})W_2^{\gamma Z}\}}{2m_H^2(s-m_Z^2)}\sin^2\theta.
\end{aligned} \tag{11}
$$

Note that $W_i^{\gamma\gamma}$, W_i^{ZZ} are real, while $W_i^{\gamma Z} = W_i^{Z\gamma *}$ can be complex. Consequently, at tree level and for real photon and Z couplings, we have $U_4 = 0$. Nonvanishing contributions to U_4 may only come from loop corrections or effective Zee-form factors.

In Secs. IV and V we discuss illustrations of SM and new physics contributions to the W_i structure functions arising in the unpolarized case, as well as in the cases of $e^{\mp}$ beams with only longitudinal or only transverse polarizations; for simplicity we restrict to real couplings. We emphasize that such illustrations apply only to X-states appearing in transitions of the type (1).

Therefore, for the formalism based on (11) to apply, special care must be taken, so that the experimental measurements assure the exclusion of X-states not generated by $\gamma, Z \to H + X$, but rather through t or u channel exchanges in $e^-e^+ \to H + X$. In the present work such X-states only appear in the SM contribution, and they are calculated directly; see Sec. IV.

A. U_1 determination through unpolarized beams

Using (10), the differential cross section for unpolarized beams may be written as

$$
\begin{aligned}
&\frac{d\sigma(e^-e^+ \to H + X)}{dp_H d\cos\theta_H} \\
&\quad = \frac{2\pi p_H^2}{p_H^0}\frac{p_H^0 d\sigma(e^-e^+ \to H + X)}{d_3 p_H},
\end{aligned} \tag{12}
$$

where only U_1 of (11) contributes. The explicit expression thus obtained consists of a constant (angular independent) term

$$
V_1 = W_1^{\gamma\gamma} + \frac{s^2(g_{Zee}^{L2} + g_{Zee}^{R2})}{2(s-m_Z^2)^2} W_1^{ZZ} - \frac{s(g_{Zee}^L + g_{Zee}^R)}{(s-m_Z^2)} W_1^{\gamma Z}, \tag{13}
$$

a term proportional to $\sin^2\theta$

$$
\begin{aligned}
V_2 &= \frac{p_H^2}{2m_H^2}\sin^2\theta\left[W_2^{\gamma\gamma} + \frac{s^2(g_{Zee}^{L2} + g_{Zee}^{R2})}{2(s-m_Z^2)^2} W_2^{ZZ}\right. \\
&\quad \left. - \frac{s(g_{Zee}^L + g_{Zee}^R)}{(s-m_Z^2)} W_2^{\gamma Z}\right],
\end{aligned} \tag{14}
$$

and a term proportional to $\cos\theta$

$$
\begin{aligned}
V_3 &= \left[\frac{s^2(g_{Zee}^{L2} - g_{Zee}^{R2})p_H\sqrt{s}}{2(s-m_Z^2)^2 m_H^2} W_3^{ZZ}\right. \\
&\quad \left. + \frac{s(g_{Zee}^R - g_{Zee}^L)p_H\sqrt{s}}{(s-m_Z^2)m_H^2} W_3^{\gamma Z}\right]\cos\theta.
\end{aligned} \tag{15}
$$

B. Longitudinally polarized beams may be used to determine U_2

Using (10), (11), this is found to consist of the angle-independent term

$$
V_4 = \frac{s^2(g_{Zee}^{L2} - g_{Zee}^{R2})}{2(s-m_Z^2)^2} W_1^{ZZ} + \frac{s(g_{Zee}^R - g_{Zee}^L)}{(s-m_Z^2)} W_1^{\gamma Z}, \tag{16}
$$

a term proportional to $\sin^2\theta$

$$
\begin{aligned}
V_5 &= \frac{p_H^2}{2m_H^2}\sin^2\theta\left[\frac{s^2(g_{Zee}^{L2} - g_{Zee}^{R2})}{2(s-m_Z^2)^2} W_2^{ZZ}\right. \\
&\quad \left. + \frac{s(g_{Zee}^R - g_{Zee}^L)}{(s-m_Z^2)} W_2^{\gamma Z}\right],
\end{aligned} \tag{17}
$$

and a term proportional to $\cos\theta$

$$
\begin{aligned}
V_6 &= \cos\theta\frac{p_H\sqrt{s}}{m_H^2}\left[\frac{s^2(g_{Zee}^{L2} + g_{Zee}^{R2})}{2(s-m_Z^2)^2} W_3^{ZZ}\right. \\
&\quad \left. - \frac{s(g_{Zee}^L + g_{Zee}^R)}{(s-m_Z^2)} W_3^{\gamma Z}\right].
\end{aligned} \tag{18}
$$

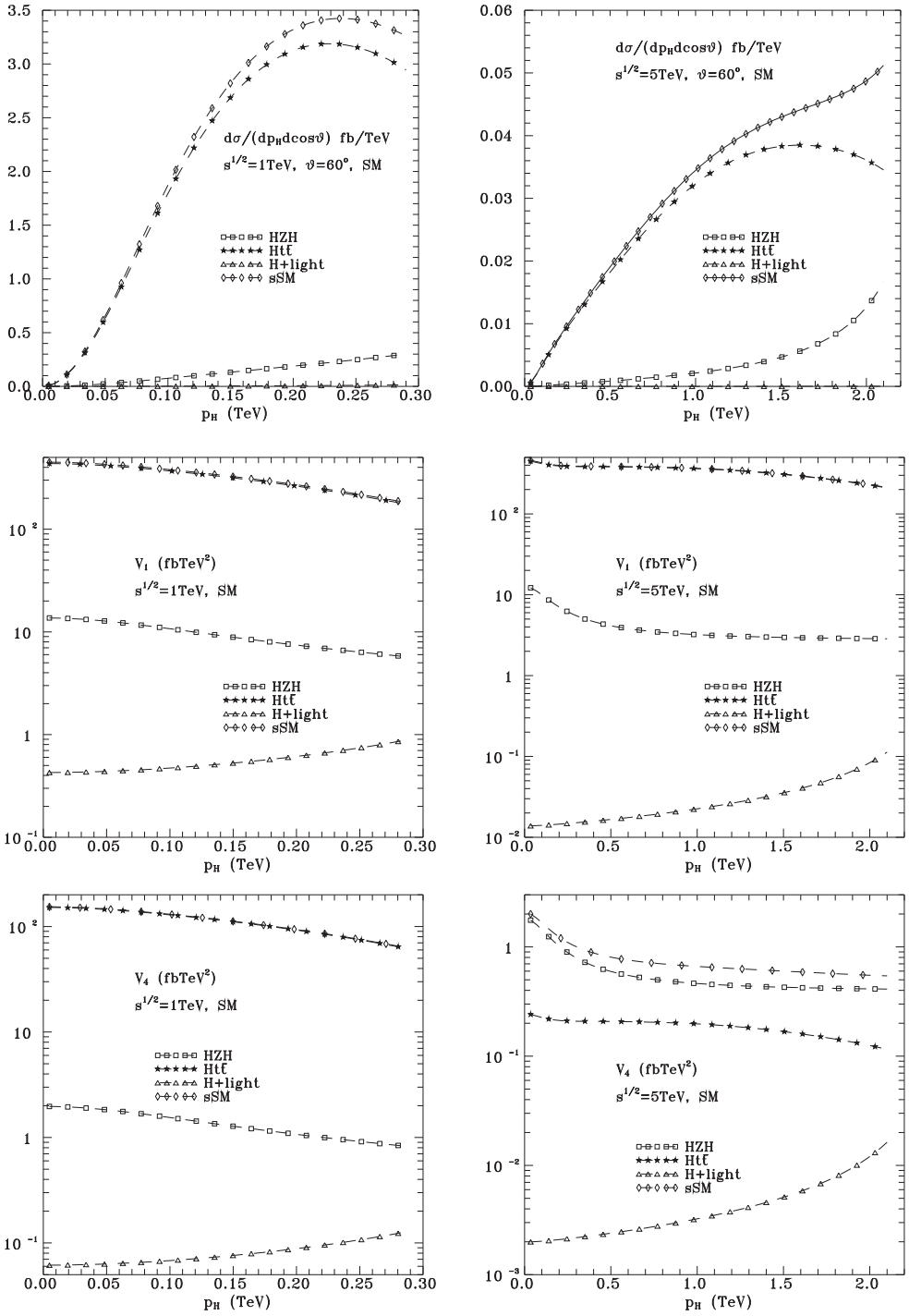

FIG. 1. Structure functions for the s-channel SM final states $X = ZH$, $X = t\bar{t}$, and the lighter quark or lepton final states $X = f\bar{f}$ called "light"; see (20). Their sum denoted as sSM is also given. Left panels correspond to $\sqrt{s} = 1$ TeV, and right panels to $\sqrt{s} = 5$ TeV. Upper panels present the differential cross section measured in fb/TeV, while middle and lower panels denote respectively V_1 and V_4 measured in fbTeV^2.

C. Transversally polarized beams may be used to determine U_3, U_4

Using again (10), (11) and real couplings so that $U_4 = 0$, the obtained cross section is fully determined by

$$V_7 = U_3 = p_H^2 \sin^2\theta \left[\frac{-W_2^{\gamma\gamma}}{2m_H^2} - 2\frac{s^2 \mathrm{Re}\{g_{Zee}^L g_{Zee}^R\}}{2m_H^2 (s-m_Z^2)^2} W_2^{ZZ} + \frac{\mathrm{Re}\{s(g_{Zee}^{L*} + g_{Zee}^{R*}) W_2^{\gamma Z}\}}{2m_H^2 (s-m_Z^2)} \right], \tag{19}$$

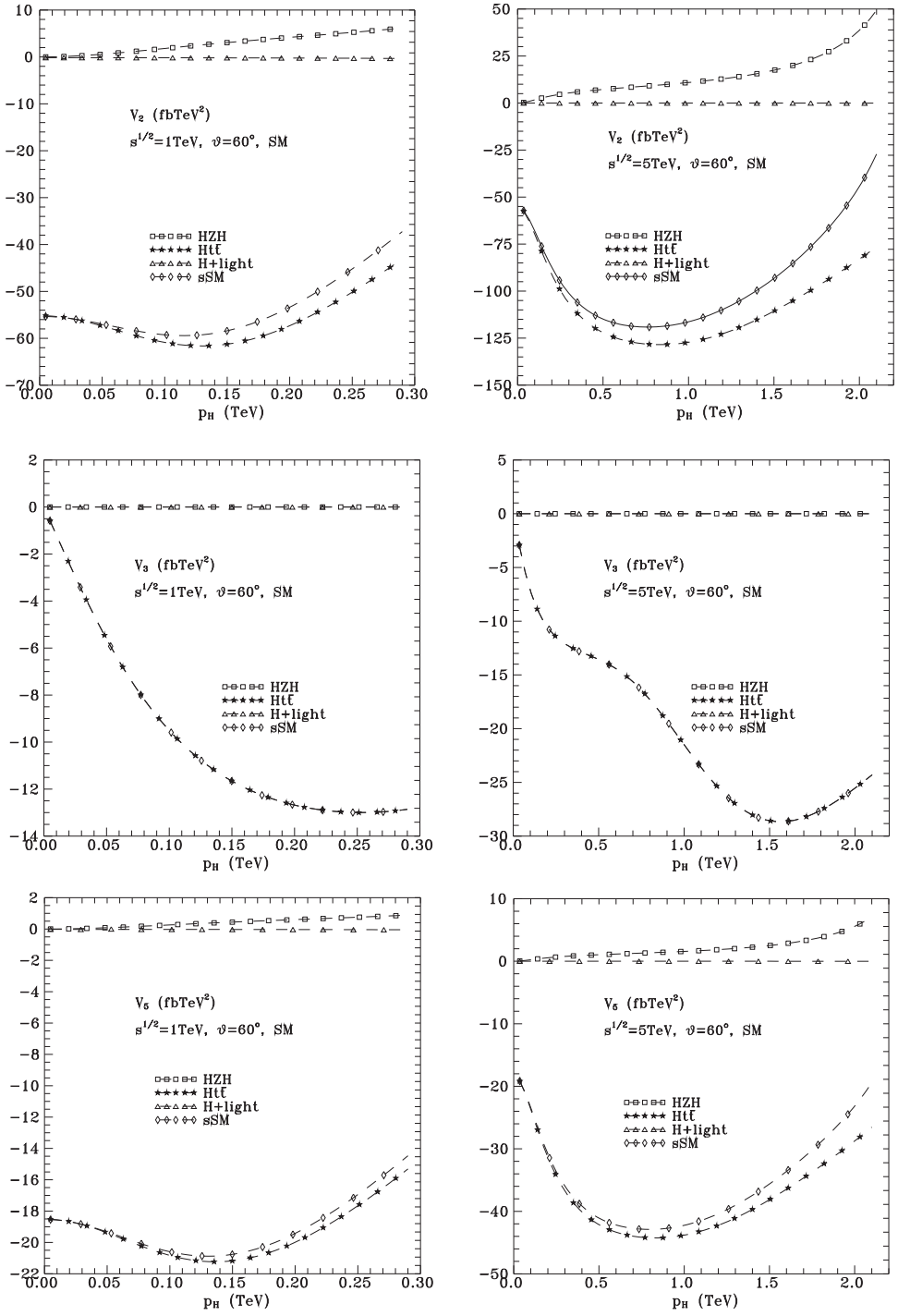

FIG. 2. s-channel SM structure functions as in Fig. 1. Upper, middle, and lower panels correspond respectively to V_2, V_3, V_5; see (14), (15), (17).

leading to a $\sin^2\theta\cos 2\phi$ angular dependence. Such a dependence should simply confirm the property of the W_2 structure functions, which of course could also be obtained from V_2, but with a different γ, Z combination.

Concerning (10)–(19), we add the following remarks:

(i) If X consists of two scalar or two vector particles, then $W_3^{\alpha\beta} = 0$. This can be seen from (4), (5) by remarking that the V and H couplings to scalar or vector particles, can never generate a parity violating I_3 contribution.

(ii) In addition, at high energy and p_H, in the scalar cases $\gamma, Z \to s + s'$ followed by $s \to H + s''$ or $s' \to H + s''$, the couplings are proportional to $p_s - p_{s'}$, so that only an I_2 contribution survives leading to $W_1^{\alpha\beta} \approx 0$.

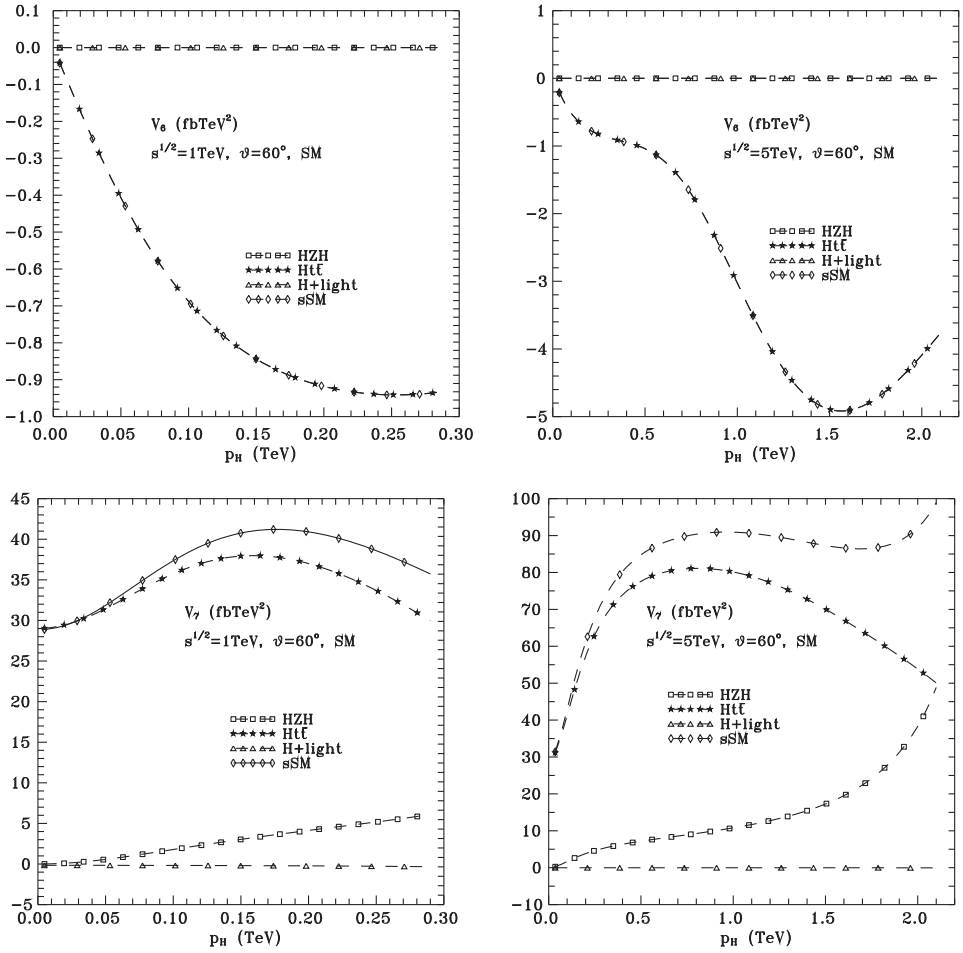

FIG. 3. s-channel SM structure functions as in Fig. 1. Upper and lower panels correspond respectively to V_6, V_7; (18), (19).

Correspondingly, in the fermion case $\gamma, Z \to f + \bar{f}$ followed by $f \to H + f$ or $\bar{f} \to H + \bar{f}$, the so-called longitudinal part $(q^\mu q^\nu)$ also vanishes when masses can be neglected in the kinematics, leading to $W_1^{\alpha\beta} + (p_H^2/m_H^2)W_2^{\alpha\beta} \approx 0$.

These properties should be useful for identifying the nature of the X states associated with the Higgs boson.

(iii) We recall that:

V_1, V_4 are combinations of $W_1^{\gamma\gamma}, W_1^{ZZ}, W_1^{Z\gamma}$,

V_2, V_5, V_7 combinations of $W_2^{\gamma\gamma}, W_2^{ZZ}, W_2^{Z\gamma}$,

V_3, V_6 combinations of $W_3^{ZZ}, W_3^{Z\gamma}$.

IV. THE H + 2-BODY CONTRIBUTIONS IN SM

A. s-channel X-forms in SM

We first concentrate on the s-channel X-forms that arise in SM through the process (1). These are

$$X = t\bar{t}, \quad f\bar{f}, \quad ZH, \tag{20}$$

where f contains all leptons and quarks except the t-one. For such X-forms the general treatment in Secs. II and III fully applies.

For each final state we compute the standard amplitude. By taking its square one obtains the $H^{\mu\nu}_{\alpha\beta}$ probability defined in Sec. II. In the $t\bar{t}$ case the amplitude is due to three diagrams

$$e^-e^+ \to \gamma, \qquad Z \to t + (\bar{t} \to \bar{t} + H), \qquad e^-e^+ \to \gamma,$$
$$Z \to \bar{t} + (t \to t + H), \quad e^-e^+ \to Z \to H + (Z \to t\bar{t})).$$

Similar diagrams occur for the light $f\bar{f}$ cases, but in this case the first two ones are negligible due to the mass suppressed $Hf\bar{f}$ coupling.

In the case of ZH one has four diagrams because the complete amplitude producing the final ZHH is symmetrized by exchange of the two Higgs-particles, before computing the probabilities and the structure functions-particles

$$e^-e^+ \to Z \to H(p_H) + (Z \to Z + H(p')),$$
$$e^-e^+ \to Z \to H(p') + (Z \to Z + H(p_H)),$$

and the other (already symmetric) ones

$$e^-e^+ \to Z \to Z + (H \to H(p_H) + H(p')),$$
$$e^-e^+ \to Z \to Z + H(p_H) + H(p'),$$

involving the 4 leg $ZZHH$ coupling.

We give in Figs. 1–3 the corresponding SM unpolarized differential cross section (12) and the structure functions $(V_1, \ldots V_7)$ appearing in (13)–(19), for each of the X states in (20). In these figures, the $X = f\bar{f}$ state is always termed as "light". In addition to them, we also give the results for the sum of all the X-sates in (20), denoted as sSM.

In all Figs. 1–3, we only give the dependencies on the Higgs momentum p_H, at a specific angle $\theta = 60°$; this angular specification is only dropped for (V_1, V_4) which are angle independent. Left panels always correspond to $\sqrt{s} = 1$ TeV, while right panels to $\sqrt{s} = 5$ TeV.

In more detail, Figs. 1 present the SM unpolarized differential cross section and the angle-independent and usually largest (V_1, V_4). Figures 2 show the angle-dependent V_2, V_3, V_5, while Figs. 3 present V_6, V_7. In all cases, the Htt contribution is the largest, then comes the ZHH one, while the light fermions contribution is much smaller.

Note also the differences in the shapes of these contributions, as well as the specific connections among the $(V_1, \ldots, V_7)$ mentioned in Sec. III. A possible violation of this may supply hints on an experimental departure from the SM predictions as we will see in the next section.

B. t- and u-channel X-forms in SM

In addition to the SM s-channel X states appearing in (20), one has to add the X-states

$$X = W^-W^+, \quad ZZ, \quad Z\gamma, \tag{21}$$

which differ by the presence of t and u channel neutrino or electron exchanges.

In the case of the $H + W^-W^+$ final state, in addition to the three s-channel diagrams

$$e^-e^+ \to \gamma, \qquad Z \to (W^- \to W^- + H) + W^+,$$
$$e^-e^+ \to \gamma, \qquad Z \to W^- + (W^+ \to W^+ + H),$$
$$e^-e^+ \to Z \to H + (Z \to W^+W^-),$$

one has the two t-channel neutrino exchange diagrams

$$e^-e^+ \to (W^- \to W^- + H) + W^+,$$
$$e^-e^+ \to W^- + (W^+ \to W^+ + H).$$

Finally, in the ZZ and $Z\gamma$ cases one has only t and u electron exchanges and one final ZZH coupling.

These t and u exchanges do not obey (1) and thus, they cannot be described in terms of the simple Higgs boson structure functions (13)–(19). Therefore, we treat them separately, and we directly compute their contributions to the inclusive cross sections $d\sigma/dp_H d\cos\theta_H$. They are illustrated in Fig. 4, as functions of p_H. In these illustrations we show the contributions of the sum of the s-channel processes given in (20) which has already appeared in the upper panels of Fig. 1 (called sSM) and in addition, we also give the contributions from the X-states in (21). The sum of all X-states in (20), (21), which describes the total SM contribution, called $\mathrm{SM_{tot}}$, is also given.

As already said, in order to analyze experimental data in terms of the simple Higgs boson structure functions (13)–(19), one has first to subtract the contributions of the X-forms in (21) from the inclusive experimental contribution to $e^-e^+ \to H + X$.

The same procedure should be applied for the ZZ and W^-W^+ fusion processes $e^-e^+ \to e^-e^+H$ and

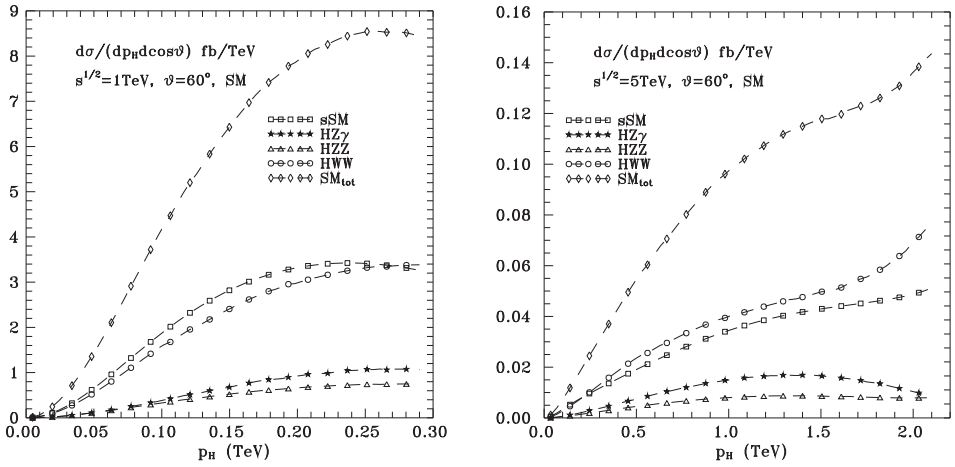

FIG. 4. The SM differential cross sections (12) from the sum of the X-channels in (20) called sSM, together with the contributions from the t- or u-channels in (21). The total contribution from all channels [(20), (21)] describes the total SM result called $\mathrm{SM_{tot}}$. Left panel corresponds to $\sqrt{s} = 1$ TeV and the right one to $\sqrt{s} = 5$ TeV.

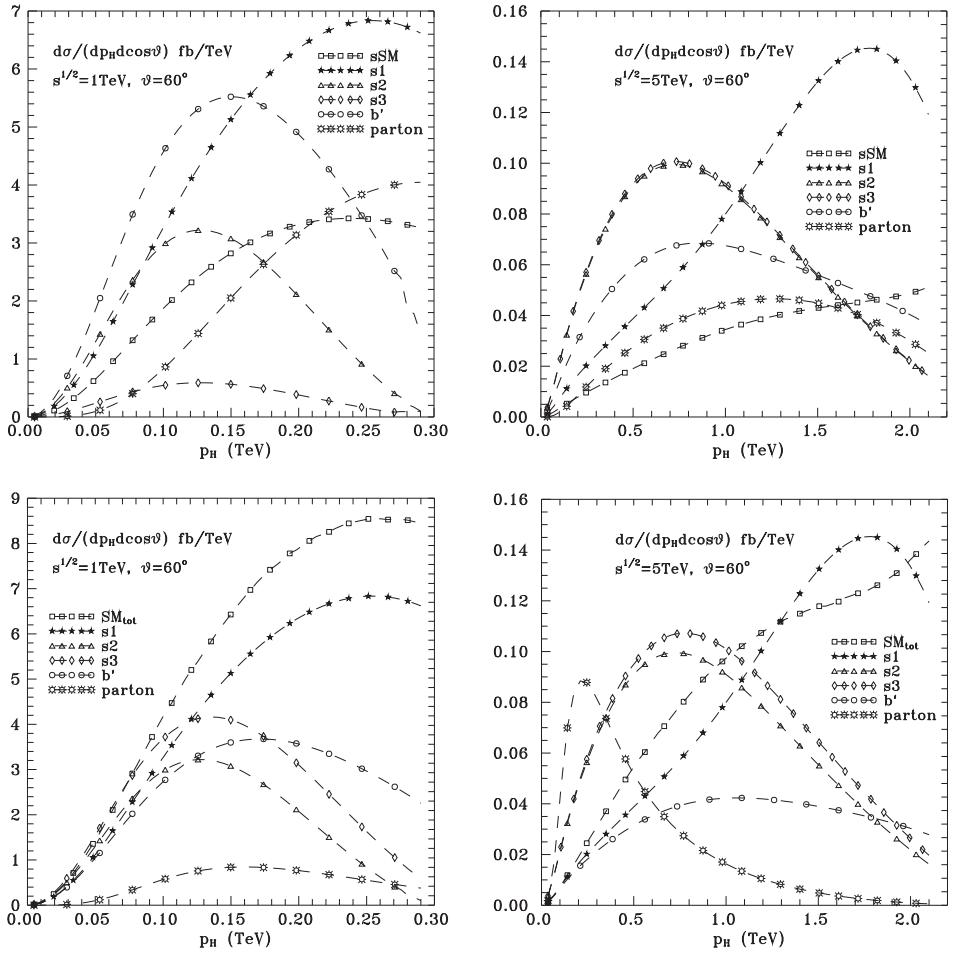

FIG. 5. The SM unpolarized differential cross sections (12) together with the new physics contributions s1, s2, s3, b', and the parton-ones discussed in Sec. V. The SM results in the upper panels only involve sSM, while those at the lower panels involve SM_{tot}; compare Figs. 4. Again, left panels correspond to $\sqrt{s} = 1$ TeV, and right panels to $\sqrt{s} = 5$ TeV.

$e^-e^+ \to \nu_e\bar{\nu}_e H$ (see [8]). *A priori* these should be added to the s-channel processes $e^-e^+ \to H + (Z \to e^-e^+, \nu_e\bar{\nu}_e)$. But, since their contribution to the H structure functions is found to be negligible, we ignore the interference of these two sets of amplitudes. One can then subtract the theoretical expectations for the fusion processes from the $e^-e^+ \to H + X$ experimental cross sections and then analyze the data according to (12), (13),…,(19) leading to Figs. 1–3.

V. NEW CONTRIBUTIONS

We now turn to possible new physics contributions. These are chosen to obey (1), so that the description in terms of the V_i in (13)–(19) remains possible. We treat the following examples:

(i) **Possible new scalar particles** s. We compute the amplitudes of the process $e^+e^- \to V \to ss$, followed by $s \to H + s$ (two diagrams). If s is neutral, then the only gauge boson it can couple to is Z. If s is charged, then it can also couple to the photon. Suitable values for the ssH-couplings are chosen, so that the overall magnitudes of the new physics effects are comparable to the SM one. The discrimination of new physics effects is then mainly based on studying the shapes of the cross section and the structure functions.

We consider three possible $s\bar{s}$-pairs, using different s-masses:

$$s1\colon\ s = \text{neutral}, \quad m_s = 0.1\ \text{TeV},$$
$$s2\colon\ s = \text{neutral}, \quad m_s = 0.28\ \text{TeV},$$
$$s3\colon\ s = \text{charged}, \quad m_s = 0.28\ \text{TeV}.$$

In all cases, we find that heavy masses give quickly a strong decrease at high p_H.

(ii) **New fermion particles** b'. The involved new physics is described by two diagrams through the processes $e^-e^+ \to V \to b'\bar{b}'$, where $V = \gamma, Z$, followed by $b' \to H + b'$ or $\bar{b}' \to H + \bar{b}'$, where b' is a new heavy b fermion. For the illustrations we choose

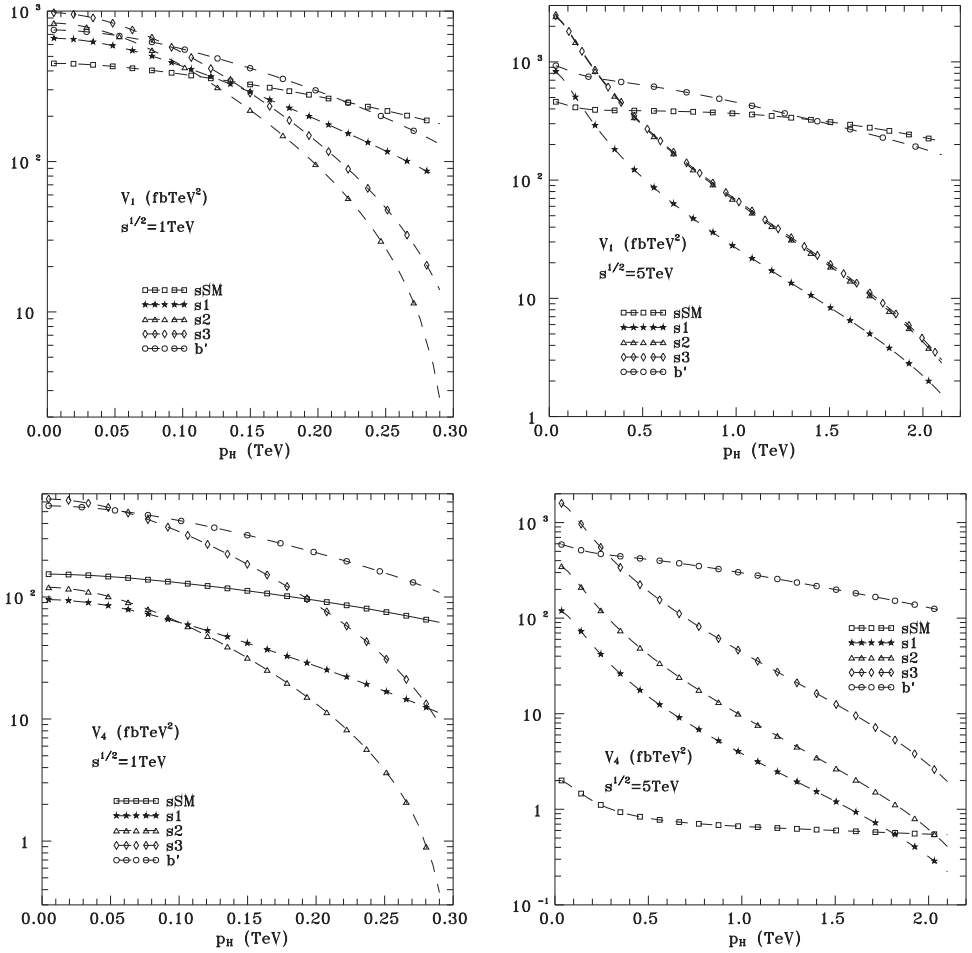

FIG. 6. Structure functions V_1 and V_4 measured in fbTeV^2, for the s-channel forms sSM (see Figs. 4), together with the new physics forms s1, s2, s3, b' and the parton contributions. Left panels correspond to $\sqrt{s} = 1$ TeV, and right panels to $\sqrt{s} = 5$ TeV.

$m_{b'} = 0.25$ TeV. This way, one may study how the distributions among the various V_i reflect the fermionic nature.

(iii) **A scalar parton model.** Another type of a schematic example could be obtained by imitating the parton model of hadronic deep inelastic scattering. Starting e.g. by assuming that transitions like $\gamma, Z \to x + x'$ exist, where x and x' are particles that may fragment to H, through transitions like $x \to H +$ "anything" and $x' \to H +$ "anything". The parton model fragmentation functions $D_x^H(z)$ and $D_{x'}^H(z)$, are modelized for example through typical $z^a(1-z)^b$ forms, with $z = 2p_H^0/\sqrt{s}$. The corresponding $W_i^{\alpha\beta}$ structure functions are then obtained by multiplying the basic $e^-e^+ \to \gamma, Z \to x + x'$ cross section by the above fragmentation functions.

Examples could be given by taking x, x' as scalars, fermions or gauge bosons and correspondingly choosing their fragmentation functions and the corresponding $W_i^{\alpha\beta}$ ones. Here we use a simple example with a neutral scalar $x = x'$ coupled to Z only. Neglecting masses for simplicity, we obtain a nonvanishing contribution only for the W_2^{ZZ}, given by[2]

$$W_2^{ZZ} = g_{Zeff}^2 \frac{8m_H^2}{sz^3} D(z), \quad \text{with} \quad D(z) = 12z(1-z). \tag{22}$$

In such a case, nonvanishing "parton" contributions are only generated for $V_{2,5,7}$. The choice $g_{Zeff}^2 \simeq 0.04$ is made in (22), so that this contribution has a magnitude comparable to the other new physics effects discussed above.

We next turn to the illustration of the above new physics effects and compare them to the related SM contributions. These are presented in Figs. 5–8. As already stated, with the choice of the new physics couplings we have made for the various models, the differences among the various new physics models we discuss are concentrated in the shapes of the various distributions.

[2]As usual, the normalization $\int_0^1 zD(z)dz = 1$ is used.

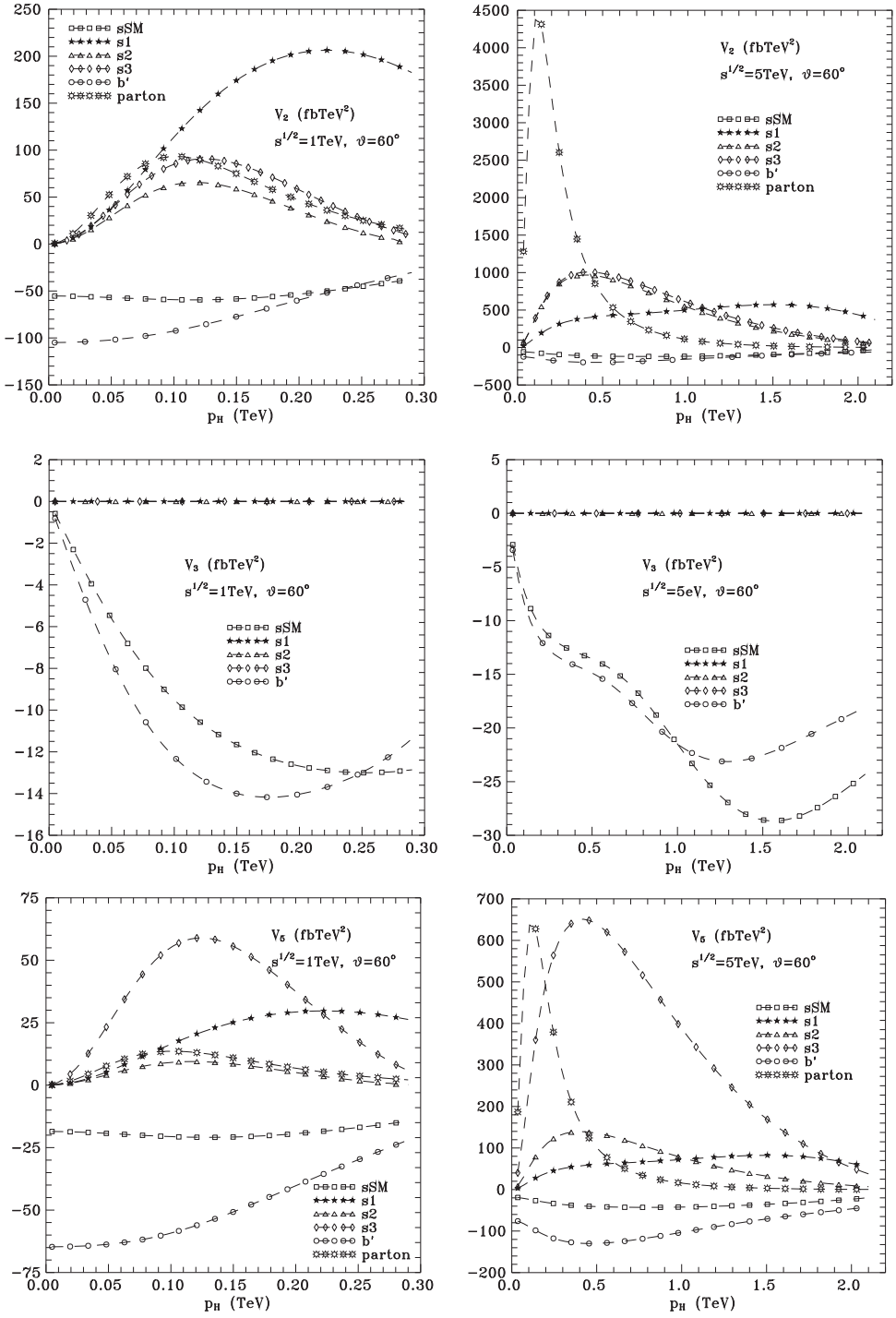

FIG. 7. As in Fig. 6, for V_2, V_3, V_5, shown respectively in the upper, middle, and lower panels.

In Figs. 5 first, we present the contributions of the scalar $s1, s2, s3$, the fermion b' and the parton model discussed above to the unpolarized differential cross sections. In addition, we also show in the upper and lower panels, the sSM (only the s-channel contributions) and SMtot (both s-channel and t,u channel contributions) standard model cases respectively. One can immediately see the differences in the shape and magnitude of the new contributions (s1, s2, s3, b', parton) with respect to those of the SM contribution, especially for high energy and p_H.

The origins of these differences can be analyzed by looking at the various V_i combinations in Figs. 6–8. The effects are much more spectacular than in the unpolarized cross section. Each new contribution gives a specific modification of the $V_{1,\ldots,7}$.

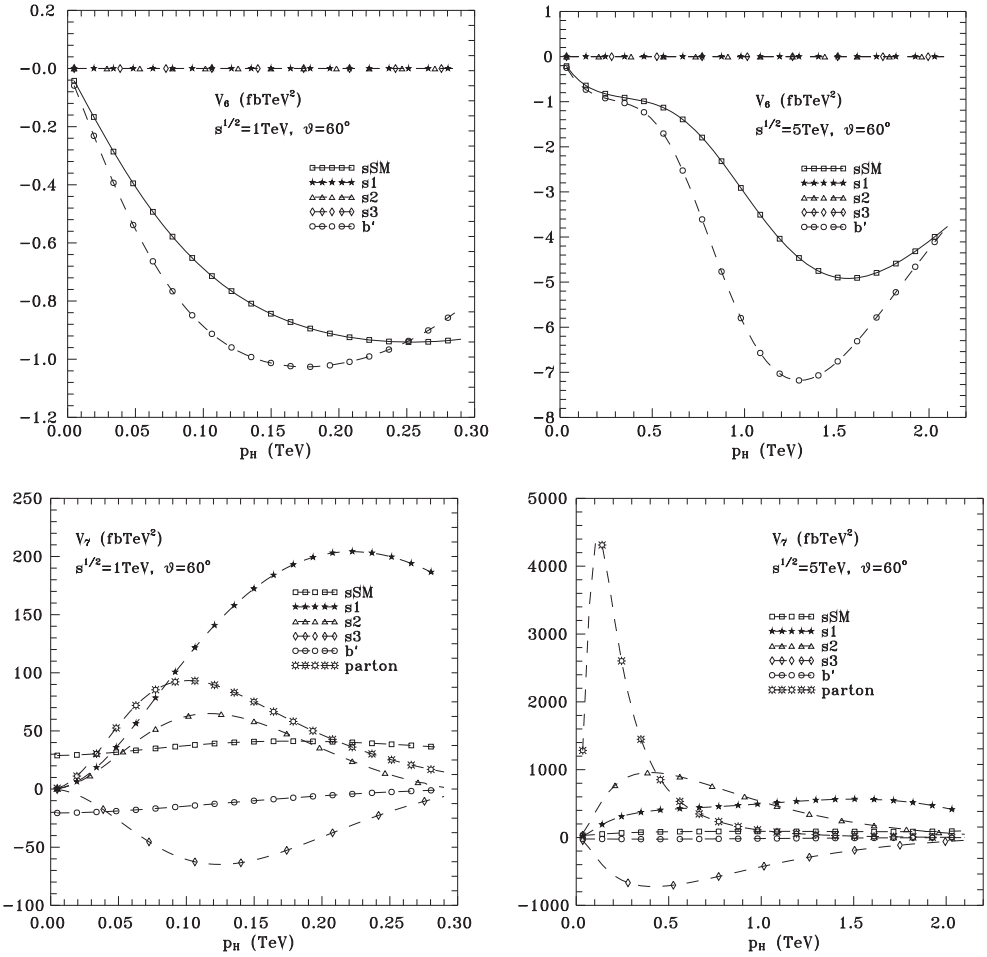

FIG. 8. As in Fig. 6, for V_6, V_7, shown respectively in the upper and lower panels.

The spin is one reason for these differences; at high energy and p_H, the scalars (including the scalar parton model) do not contribute to $V_{1,3,6}$. The masses are another reason, as one can see by comparing the shapes of $s1$ and $s2, s3$. This feature could be useful for identifying invisible matter.

In more detail, Figs. 6 present the angular independent structure functions V_1, V_4 as functions of p_H. These are usually the largest and they are positive for all p_H. In contrast to them, the structure functions V_2, V_3, V_5 (Figs. 7) and V_6, V_7 (Figs. 8) may change sign as p_H varies, and are usually considerably smaller. Exceptions appear for the parton contributions at $\sqrt{s} = 5$ TeV and low p_H, for V_2, V_5, V_7; and also for the s3-contribution to V_5 at $p_H \sim 0.5$ TeV.

VI. CONCLUSIONS AND POSSIBLE FUTURE DEVELOPMENTS

In this paper we propose an analysis of the Higgs boson structure functions in e^-e^+ collisions.

In doing so, we have first computed the theoretical expectations for the SM contributions to these structure functions and to their combinations appearing in the angular terms of the inclusive cross section $e^-e^+ \to H+$ "anything". We have then given examples of possible new particle contributions and examined how they modify the shapes of the distributions of the various Higgs boson structure functions, such that one can suspect what type of new particles are produced, without observing them.

These differences arise from the spins, masses and couplings of the new particles involved, and reflect in the p_H dependencies and the signs and magnitudes of the various W_i or of their effective combinations V_i. They are rather spectacular, first in the global unpolarized differential cross sections and more drastically in the various V_i combinations controlling its angular components (see illustrations). The shapes of these distributions may allow to guess what type of new particle (spin, mass) is responsible of a departure from SM when it is observed, even if this particle is not visible.

Our conclusion is then the following: the shapes of the Higgs boson structure functions can tell us something about new physics.

The output of this first work is essentially a suggestion for further more detailed phenomenological and experimental

studies. Obviously several improvements could be performed like a complete treatment including higher orders and background processes.

There should also be the possibility of studies of other inclusive processes. The closest one to the case considered in the present work being for example $q\bar{q} \to H +$ "anything", in particular $q\bar{q}' \to W \to H +$ "anything" at LHC. But other processes, for example with initial photons or gluons, $\gamma\gamma \to H +$ "anything", $gg \to H +$ "anything" could also be considered.

[1] G. Aad *et al.* (ATLAS Collaboration), Phys. Lett. B **716**, 1 (2012); S. Chatrchyan *et al.* (CMS Collaboration), Phys. Lett. B **716**, 30 (2012); G. J. Davies (CDF and D0 Collaborations), Front. Phys. China **8**, 270 (2013); ATLAS Collaboration, https://twiki.cern.ch/twiki/bin/view/AtlasPublic/HiggsPublicResults. CMS Collaboration: https://twiki.cern.ch/twiki/bin/view/CMSPublic/PhysicsResultsHIG.

[2] P. Higgs, Phys. Lett. **12**, 132 (1964); Phys. Rev. Lett. **13**, 508 (1964); Phys. Rev. **145**, 1156 (1966); F. Englert and R. Brout, Phys. Rev. Lett. **13**, 321 (1964); G. Guralnik, C. Hagen, and T. Kibble, Phys. Rev. Lett. **13**, 585 (1964).

[3] J. Ellis, arXiv:1312.5672; S. Dawson *et al.* (Higgs Working Group), arXiv:1310.8361, M. Klute, R. Lafaye, T. Plehn, M. Rauch, and D. Zerwas, Europhys. Lett. **101**, 51001 (2013). A. Djouadi, Phys. Rep. **459**, 1 (2008); J. Gunion, H. Haber, G. Kane, and S. Dawson, *The Higgs Hunter's Guide* (Addison-Wesley, Reading, MA, 1990); S. Heinemeyer, Int. J. Mod. Phys. A **21**, 2659 (2006).

[4] E. Massó, J. High Energy Phys. 10 (2014) 128; E. Massó and V. Sanz, Phys. Rev. D **87**, 033001 (2013); H. Bélusca-Maïto, arXiv:1507.05657; For an introduction on the connections between the muon $g-2$ and dark matter, see, e.g., G. Bélanger, C. Delaunay, and S. Westhoff, arXiv:1507.06660.

[5] M. E. Peskin, arXiv:1506.08185v3; M. Muhlleitner, arXiv:1410.5093; Ben Gripaios, arXiv:1503.02636; arXiv:1506.05039.

[6] B. Patt and F. Wilczek, hep-ph/0605188.

[7] F. M. Renard, *Basics Of Electron Positron Collisions* (Editions Frontières, Gif sur Yvette, France, 1981).

[8] K. Fujii *et al.*, arXiv:1506.05992v2; G. Moortgat-Pick *et al.*, Eur. Phys. J. C **75**, 371 (2015).